Original scientific paper
https://doi.org/10.33180/InfMIDEM2022.204

Informacije MIDEM
Journal of Microelectronics,
Electronic Components and Materials
Vol. 52, No. 2(2022), 105 – 115

Electronically Tunable Mixed Mode Universal Filter Employing Grounded Passive Components

Ramesh Mishra[1], Ganga Ram Mishra[2], Shri Om Mishra[1] , Mohammad Faseehuddin[3]

[1]Department of Physics and Electronics, Dr. Rammanohar Lohia Avadh University Ayodhya U.P., India
[2]Department of Physics & Electronics, Dr. Rammanohar Lohia Avadh University, India
[3]Department of Electronics and Telecommunication, Symbiosis Institute of Technology (SIT), Symbiosis International University (SIU), Lavale, Mulshi, Pune, Maharashtra, India

Abstract: A recently developed active element, namely Voltage Differencing Differential Voltage Current Conveyor (VD-DVCC), is employed in the design of electronically tunable mixed-mode universal filter. The filter provides low pass (LP), high pass (HP), band pass (BP), band reject (BR) and all pass (AP) responses in voltage-mode (VM), current-mode, trans-impedance-mode (TIM) and trans-admittance-mode (TAM). The filter employs two VD-DVCCs, three resistors and two capacitors. All the passive components employed are grounded. The attractive features of the filters include: (i) ability to operate in all four modes, (ii) use of grounded passive components, (iii) tunability of Q factor independent of pole frequency, (iv) high input impedance for VM and TIM mode, (v) high output impedance explicit current output for CM and TAM and (vi) no requirement for double/negative input signals (voltage/current) for response realization. The VD-DVCC is designed and validated in Cadence virtuoso using 0.18 µm PDK at supply voltage of ±1 V. The operation of filter is examined at 5.305 MHz frequency. The non-ideal gain and sensitivity analysis is also carried out to study the effect of process and components spread on the filter performance. The obtained results bear close resemblance with the theoretical findings.

Keywords: communication, mixed-mode, current conveyor, filter, signal processing, VD-DVCC

Elektronsko nastavljiv univerzalni filter mešanega načina z ozemljenimi pasivnimi komponentami

Izvleček: Nedavno razviti aktivni element napetostni diferenčni napetostni tokovni transporter (VD-DVCC) je uporabljen pri zasnovi elektronsko nastavljivega univerzalnega filtra z mešanim načinom delovanja. Filter omogoča nizko prepustnost (LP), visoko prepustnost (HP), pasovno prepustnost (BP), pasovno zavrnitev (BR) in vse prepustne odzive (AP) v napetostnem (VM), tokovnem, trans-impedančnem (TIM) in trans-admitančnem (TAM) načinu. Filter uporablja dva VD-DVCC, tri upore in dva kondenzatorja. Vse uporabljene pasivne komponente so ozemljene. Privlačne lastnosti filtrov so: (i) možnost delovanja v vseh štirih načinih, (ii) uporaba ozemljenih pasivnih komponent, (iii) nastavljivost faktorja Q neodvisno od frekvence polov, (iv) visoka vhodna impedanca za način VM in TIM, (v) visoka izhodna impedanca z eksplicitnim izhodnim tokom za CM in TAM ter (vi) ni potrebe po dvojnih/negativnih vhodnih signalih (napetost/tok) za realizacijo odziva. VD-DVCC je zasnovan in preverjen v Cadence virtuoso z uporabo 0,18 µm PDK pri napajalni napetosti ±1 V. Delovanje filtra je preverjeno pri frekvenci 5,305 MHz. Izvedena je tudi analiza neidealnega ojačenja in občutljivosti, da bi preučili vpliv razpršenosti procesa in komponent na delovanje filtra. Dobljeni rezultati so zelo podobni teoretičnim ugotovitvam.

Ključne besede: komunikacija, mešani način, tokovni transporter, filter, obdelava signalov, VD-DVCC

** Corresponding Author's e-mail: rameshmishra1985@gmail.com*

1 Introduction

The current mode-active elements (CM-AEs) are extensively employed in designing universal frequency filters [1-4]. The CM-AEs exhibits enhanced dynamic range, wide bandwidth, simple structure, low power consumption and greater linearity [2-3]. Numerous filter structures employing CM-AEs can be found in the literature [1, 3]. Most of the proposed filters can work

How to cite:
R. Mishra et al., "Electronically Tunable Mixed Mode Universal Filter Employing Grounded Passive Components", Inf. Midem-J. Microelectron. Electron. Compon. Mater., Vol. 52, No. 2(2022), pp. 105–115

only in single mode of operation i.e. voltage-mode (VM), current-mode (CM), trans-admittance-mode (TAM), and trans-impedance-mode (TIM) [1-3,5]. In present day complex signal processing systems, the interaction between CM and VM circuits is required. This task can be performed by TAM and TIM filters that not only perform signal processing, but also provide interfacing between VM and CM systems [6-10]. The development of mixed-mode universal filters that can provide LP, HP, BP, BR and AP responses in CM, VM, TAM and TIM modes of operation are best suited for the task.

Numerous exemplary mixed-mode filter topologies have been developed [6-41] that employ CM-AEs. The mixed mode filters can be categorised into two groups (i) single input multi output (SIMO), (ii) multi input single output (MISO) structures. The filter structures [6-10**,** 12-13, 15-19, 22-24, 28, 31-33, 35, 37-39, 41] employ CM-AEs in excess of two. The designs in [6-7, 10,12,22,28-30, 36, 37, 39] employ more than five passive components. The filter structures in [6, 7, 10-12, 14, 20-22, 25, 27-30, 34, 36, 39, 48-52] does not employ all grounded passive components. The filters in [6-7, 9-13, 18, 19, 21, 24, 25, 27, 30, 32, 33, 36, 39] do not provide frequency control independent of quality factor. The filter topologies [6, 8, 9, 11, 13, 15, 16, 18, 21, 23, 25, 26-28, 32, 34, 41, 50] do not provide all five filter responses in VM, CM, TAM, and TIM operation. The filter structures [6, 7, 10-12, 14, 16, 22, 25, 27-30, 34, 36, 37, 39, 41] lack inbuilt tunability. Some recent designs of the mixed mode filters proposed by the authors [48-52] suffer from one or more of the above discussed drawbacks. A detailed comparison of the state-of-the-art MISO filters with the proposed design is presented in Table 1, based on the following important measures of comparison: (i) number of CM-AEs employed, (ii) number of passive components needed, (iii) employment of all grounded passive components, (iv) no requirement for resistive matching except for obtaining a single response, (v) provision to control quality factor (*Q*) independent of the centre frequency, (vi) ability to provide all five filter responses in all four modes of operation, (vii) low output impedance for VM and TIM modes, (viii) availability of explicit current output in CM and TAM, (ix) no requirement for double/negative input signals (voltage/current), (x) inbuilt tunability, and (xi) test frequency.

It can be inferred from the literature review and table 1 that not all the proposed mixed mode filter structures work in all four modes of operation. It is also deduced from the literature survey that limited number of mixed-mode filters are available and to fill this technological void additional novel mixed-mode filter structures are needed. In this research, a recently developed CM-AE, the Voltage Differencing Differential Voltage Current Conveyor (VD-DVCC) is utilized in design of mixed-mode filter. The design requires two VD-DVCCs, two capacitors, and three resistors. The striking features of the proposed filter are: (i) ability to work in all four modes of operation, (ii) provision for inbuilt tunability, (iii) the filters enjoy low active and passive sensitivities, and (iv) use of all grounded passive components. Beside these the filters enjoy all the properties mentioned in Table 1 except (vii). The design and simulation of the VD-DVCC is done in Cadence Virtuoso using 0.18µm PDK. The simulation results bear close resemblance with the theoretical findings.

2 Voltage differencing differential voltage current conveyor (VD-DVCC)

The VD-DVCC is a newly proposed [42] CM-AE that possess features of Differential Voltage Current Conveyor (DVCC) [41] and Operational Transconductance Amplifier (OTA). The voltage current relations of the VD-DVCC are given in Equations (1)-(4) and the block diagram is shown in Figure 1.

$$I_W = I_{WC+} = -I_{WC-} = g_m\left(V_P - V_N\right) \tag{1}$$

$$V_X = V_{Y1} - V_W \tag{2}$$

$$I_X = I_{Z+} = -I_{Z-} \tag{3}$$

$$I_{Y1} = I_w = 0 \tag{4}$$

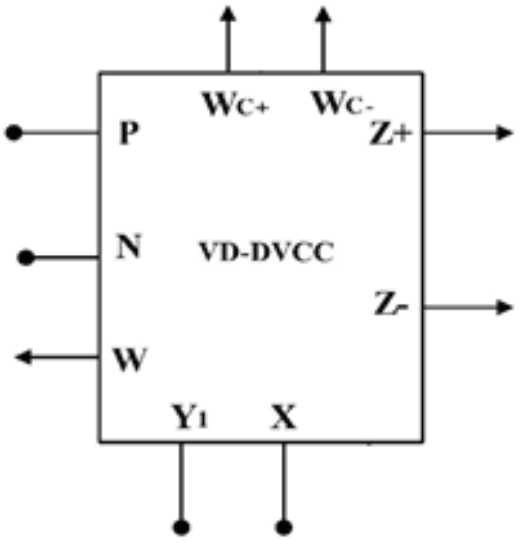

Figure 1: Block Diagram of VD-DVCC

The CMOS implementation of VD-DVCC is presented in Figure 2. The transistors M19-M32 forms the OTA section. The output current of the OTA assuming all tran-

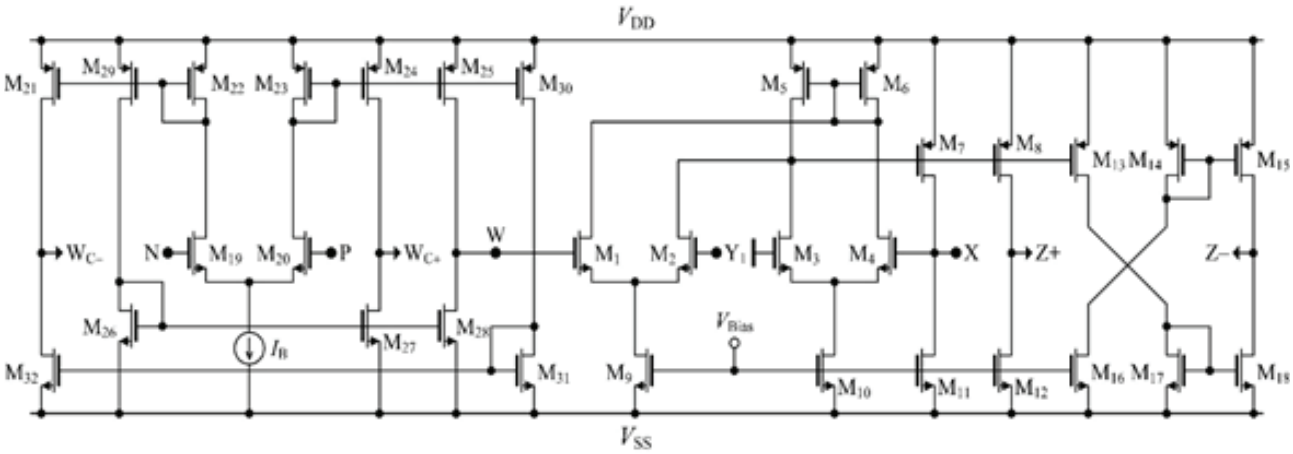

Figure 2: CMOS implementation of VD-DVCC

sistors in saturation region and equal width and length for (M19-M20) will be $I_W = I_{WC} = g_m(V_P - V_N)$. The expression for g_m is given in Equation 5.

$$g_m = \sqrt{\mu_n C_{OX} \frac{W}{L} I_B} \tag{5}$$

Where C_{OX} is the gate oxide capacitance, μ_n is the mobility of electrons in NMOS, g_m denotes the transconductance of OTA set via bias current I_B and W/L is the aspect ratio of the transistors. Extra copies of the OTA current can be utilized, if necessary, for the applications. The second stage comprising of transistors M1-M18 provides algebraic summation of input voltages and current transfer function. The voltage at the X terminal is the algebraic sum of voltages at W and Y_1 terminals. The input current at the X terminal appears at the Z+ and Z- terminals, multiple copies of the current can be easily generated just by adding two extra transistors. The N, P, Y_1 terminals are high impedance voltage input terminals. The W, W_{C+}, W_{C-}, Z + and Z - are high impedance current output terminals. The X terminal is low impedance current input terminal.

3 Proposed electronically tunable mixed-mode universal filter

The proposed filter as presented in Figure 3 requires two VD-DVCCs, two capacitors, and three resistors all grounded for the design. For VM and TAM mode of operation the filter has high input impedance. In addition, the CM and TAM responses are available from explicit high impedance terminals. Furthermore, in the design the capacitors are connected to high impedance terminals so they will absorb the parasitic associated with the terminals. Among the three resistors two are connected to the low resistance X terminal so they will accommodate the parasitic resistance present at X terminal. The important features of the filter include: (i) use of grounded passive components, (ii) employment of minimum number of passive components, (iii) no need for capacitive matching, (iv) no requirement for resistive matching except for AP response, (v) high input impedance in VM and TIM configuration, (vi) ability to provide all five filter responses in all four modes of operation, (vii) availability of explicit current output in CM and TAM, (viii) no requirement for double/negative input signals (voltage/current), and (xi) inbuilt tunability. The operation of the filter in all modes is explained below.

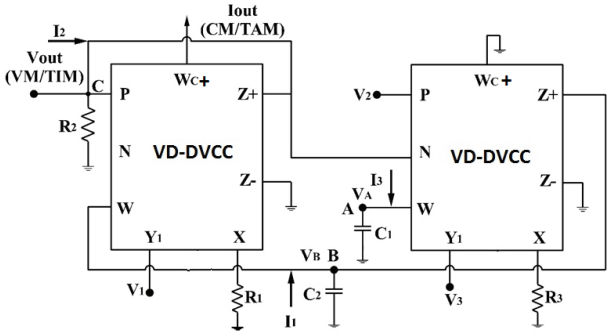

Figure 3: Proposed Mixed-mode Filter

3.1 Operation in VM and TAM mode:

In this mode of operation, the inputs currents ($I_1 - I_3$) are set to zero. The filter is excited with input voltages ($V_1 - V_3$) as per the sequence given in Table 2. The Equations (10-11) give the filter response in VM and TAM modes of operation. The frequency and quality factor are given by Equations (12-13). It can be deduced from the Equations that the Q can be controlled independent of frequency. For all pass response a simple resistive matching of ($R_1 = R_2$) is required which is easy to achieve.

$$V_{out} = \frac{s^2 C_1 C_2 R_2 R_3 V_1 - SC_1 R_2 V_3 + R_2 g_{m2} V_2}{s^2 C_1 C_2 R_1 R_3 + g_{m1} SC_1 R_3 R_2 + R_2 g_{m2}} \quad (10)$$

In Equation 10 the filter gain constants are $H_{oLP} = 1$, $H_{oHP} = \frac{R_2}{R_1}$, $H_{oBP} = g_1 R_2$ by adjusting these parameters the filter gain can be adjusted. As special case for notch pass or bad reject realization if $R_2 > R_1$ then high pass notch (HPN) is obtained and if $R_2 < R_1$ low pass notch (LPN) response is obtained.

$$I_{out\,(TAM)} = g_{m1} V_{out}$$

$$I_{out\,(TAM)} = g_{m1}\left[\frac{s^2 C_1 C_2 R_2 R_3 V_1 - SC_1 R_2 V_3 + R_2 g_{m2} V_2}{s^2 C_1 C_2 R_1 R_3 + g_{m1} SC_1 R_3 R_2 + R_2 g_{m2}}\right] \quad (11)$$

$$f_o = \frac{1}{2\pi}\sqrt{\frac{g_{m2} R_2}{C_1 C_2 R_1 R_3}} \quad (12)$$

$$Q = \frac{1}{g_{m1}}\sqrt{\frac{C_2 g_{m2} R_1}{C_1 R_2 R_3}} \quad (13)$$

Table 1: Excitation Sequence for VM and TAM

Response	Inputs			Matching Condition
	V_1	V_2	V_3	
LP	0	1	0	No
HP	1	0	0	No
BP	0	0	1	No
BR	1	0	1	No
AP	1	1	1	$R_1 = R_2$, $R_3 g_1 = 1$

3.2 Operation in CM and TIM mode:

In this mode of operation all input voltages () are set to zero. The input currents () are applied according to Table 3. The transfer function for CM and TIM are given in Equations (14)-(15). The complete analysis of the circuit is given below.

$$V_{out(TIM)} = \left[\frac{s^2 C_1 C_2 R_1 R_3 R_2 I_2 - SC_1 R_3 R_2 I_1 + R_2 I_3}{s^2 C_1 C_2 R_1 R_3 + g_{m1} SC_1 R_3 R_2 + R_2 g_{m2}}\right] \quad (14)$$

$$I_{out\,(CM)} = g_{m1} V_{out}$$

$$I_{out(CM)} = \left[\frac{s^2 C_1 C_2 R_1 R_3 g_{m1} R_2 I_2 - SC_1 R_3 g_{m1} R_2 I_1 + g_{m1} R_2 I_3}{s^2 C_1 C_2 R_1 R_3 + g_{m1} SC_1 R_3 R_2 + R_2 g_{m2}}\right] \quad (15)$$

In Equation 15 the filter gain constants are $H_{oLP} = \frac{g_1}{g_2}$, $H_{oHP} = g_1 R_2$, $H_{oBP} = 1$ by adjusting these parameters the filter gain can be adjusted.

Table 3: Input current excitation sequence

Response	Inputs			Matching Condition
	I_1	I_2	I_3	
LP	0	0	1	No
HP	0	1	0	No
BR	1	0	0	No
NP	0	1	1	No
AP	1	1	1	$g_1 R_2 = 1$, $g_1 = g_2$

4 Non-Ideal and Sensitivity Analysis

The non-ideal model of the VD-DVCC is given in Figure 5. As can be deduced, various parasitic resistance and capacitance appear in parallel with the input and output nodes of the device. The low impedance X node has a parasitic resistance and inductance in series with it. Other non-ideal effects that influence the response of the VD-DVCC are the frequency dependent non-ideal current (), voltage (), and transconductance transfer (γ, γ′) gains. These non-ideal gains result in a change in the current and voltage signals during transfer leading to undesired response. Taking in account the non-ideal gains the V-I characteristics of the VD-DVCC in (1) will be modified as follows: $I_W = 0$, $V_X = \beta(V_1 - V_W)$, $I_{Z+} = \alpha_P I_X$, $I_{Z-} = \alpha_N I_X$, $I_W = I_{WC+} = \gamma g_m (V_p - V_N)$, $I_{WC-} = -\gamma' g_m (V_p - V_N)$ where $\beta_m = 1 - \varepsilon_{vm}$, $\alpha_{Pm} = 1 - \varepsilon_{iPm}$, $\alpha_{Nm} = 1 - \varepsilon_{iNm}$, $\gamma_m = 1 - \varepsilon_{gmm}$, (***drugi m subsub***) and $\gamma'_m = 1 - \varepsilon'_{gmm}$ (***drugi m subsub***) for m = 1, 2, which refers to the number of VD-DVCCs. Here, ε_{vm} ($|\varepsilon_{vm}| \ll 1$) denote voltage tracking error, ε_{iPm}, ε_{iNm} ($|\varepsilon_{im}|$, $|\varepsilon_{iNm}| \ll 1$) denote current tracking errors, and ε_{gmm}, ε'_{gmm} ($|\varepsilon_{gmm}|$, $|\varepsilon'_{gmm}| \ll 1$) (***drugi m subsub***) denote transconductance errors of the VD-DVCC.

The non-ideal analysis considering the effect of non-ideal current, voltage, and transconductance transfer gains is carried out for MISO (VM, CM, TAM and TIM) configurations to see its effect on the transfer function, f_0, and Q of the proposed filters. The modified expressions of filter transfer functions, f_0', and Q′ for the MISO configuration are presented in Equations (16)-(21).

Table 2: Comparative study of the state-of-the-art MISO Mixed mode filter designs with the proposed filter

References	Mode of Operation	(i)	(ii)	(iii)	(iv)	(v)	(vi)	(vii)	(viii)	(ix)	(x)	(xi)
[9]/2003	MISO	6-OTA	2C	Yes	Yes	No	No	No	Yes	Yes	Yes	-
[7]/2004	MISO	7-CCII	2C+8R	No	Yes	No	Yes	No	Yes	Yes	No	-
[12]/2006	MISO	3-CCII	3C+4R+ 2-switch	No	No	No	Yes	No	Yes	Yes	No	-
[13]/2008	MISO	4-OTA	2C	Yes	Yes	No	No	No	Yes	Yes	Yes	2.25 MHz
[19]/2010	MISO	5-OTA	2C	Yes	Yes	No	Yes	No	Yes	No	Yes	1.59 MHz
[20]/2010	MISO	2-MOCCCII	2C+2R	No	Yes	Yes	Yes	No	Yes	Yes	Yes	1.27 MHz
[27]/2010	MISO	CFOA	2C+3R	No	No	Yes	No	No	Yes	No	No	12.7MHz
[24]/2013	MISO	4-MOCCCII	2C	Yes	Yes	No	Yes	Yes	Yes	No	Yes	-
[25]/2013	MISO	1-FDCCII	2C+2R	No	Yes	No	No	No	Yes	Yes	No	10 MHz
[26]/2013	MISO	2-VDTA	2C	Yes	Yes	Yes	No	No	Yes	Yes	Yes	1 MHz
[29]/2016	MISO	1-FDCCII+1-DDCC	2C+6R	No	Yes	Yes	Yes	No	Yes	No	No	1.59 MHz
[37]/2018	MISO	5-DVCC	2C+5R	Yes	Yes	Yes	Yes	No	Yes	Yes	No	1MHz
[40]/2018	MISO	4-CCII	2C+4R	Yes	Yes	Yes	No	No	Yes	Yes	No	31.8 MHz
[38]/2019	MISO	5-OTA	2C	Yes	Yes	Yes	Yes	No	Yes	Yes	Yes	3.390 MHz
[39]/2020	MISO	3-DDCCII	2C+4R	No	Yes	No	Yes	No	Yes	Yes	No	3.978 MHz
[48]/2020	MISO/SIMO	2-EXCCTA	2C+4R	No	Yes	Yes	Yes	No	Yes	Yes	Yes	7.622 MHz
[49]/2021	MISO	2-VD-DVCC	2C+3R	No	Yes	Yes	Yes	No	Yes	Yes	Yes	5.305 MHz
[50]/2021	MISO	2-VDBA	2C+2R	No	Yes	Yes	No	Yes	No	Yes	Yes	1.52 MHz
[51]/2021	MISO	3-VDBA	2C+R	No	Yes	Yes	Yes	Yes	Yes	Yes	Yes	16.631 MHz
[52]/2022	MISO	1-VD-EXCCII	2C+2R	No	Yes	Yes	Yes	No	Yes	Yes	Yes	8.08 MHz
This Works	MISO	2-VD-DVCC	2C+3R	Yes	Yes	Yes	Yes	No	Yes	Yes	Yes	5.305 MHz

** Full nomenclature of the mentioned CM-AEs in Tables 1 and 2 in alphabetical order: CCCCTA: Current controlled current conveyor transconductance amplifier, CCII: Second-generation current conveyor, CFOA: Current feedback operational amplifier, DDCC: Differential difference current conveyor, DPCCII: Digitally programmable second-generation current conveyor, DVCC: Differential voltage current conveyor, EXCCTA: Extra X current conveyor differential input transconductance amplifier, FDCCII: Fully differential second-generation current conveyor, FTFN: Four terminal floating nullor, ICCII: Inverting second-generation current conveyor, MOCCCII: Multi output current controlled current conveyor, MOCCII: Multi output second-generation current conveyor, OTA: Operational transconductance amplifier, VDTA: Voltage differencing transconductance amplifier, VDBA: Voltage differencing buffered amplifier, VD-EXCC: Voltage differencing extra X current conveyor*

$$V'_{out(VM-Mode)} = \left[\frac{s^2 C_1 C_2 R_2 R_3 \alpha_{P1} \beta_1 V_1 - S C_1 R_2 \alpha_{P2} \beta_2 \alpha_{P1} \beta_1 V_3 + \alpha_{P2} \beta_2 \gamma_2 g_{m2} R_2 g_2 V_2}{s^2 C_1 C_2 R_1 R_3 + g_{m1} S C_1 R_3 R_2 \alpha_{P1} \beta_1 \gamma_1 + \alpha_{P2} \beta_2 \gamma_2 \alpha_{P1} \beta_1 R_2 g_{m2}} \right] \tag{16}$$

$$I'_{out(TAM-Mode)} = \gamma_1 g_{m1} \left[\frac{s^2 C_1 C_2 R_2 R_3 \alpha_{P1} \beta_1 V_1 - S C_1 R_2 \alpha_{P2} \beta_2 \alpha_{P1} \beta_1 V_3 + \alpha_{P2} \beta_2 \gamma_2 g_2 R_2 g_{m2} V_2}{s^2 C_1 C_2 R_1 R_3 + g_{m1} S C_1 R_3 R_2 \alpha_{P1} \beta_1 \gamma_1 + \alpha_{P2} \beta_2 \gamma_2 \alpha_{P1} \beta_1 R_2 g_{m2}} \right] \tag{17}$$

$$I'_{out(CM-Mode)} = \gamma_1 g_{m1} \left[\frac{s^2 C_1 C_2 R_1 R_3 R_2 I_2 - S \alpha_{P1} \beta_1 C_1 R_3 R_2 I_1 + R_2 \alpha_{P1} \beta_1 \alpha_{P2} \beta_2 I_3}{s^2 C_1 C_2 R_1 R_3 + g_{m1} S C_1 R_3 R_2 \alpha_{P1} \beta_1 \gamma_1 + \alpha_{P2} \beta_2 \gamma_2 \alpha_{P1} \beta_1 R_2 g_{m2}} \right] \tag{18}$$

$$V'_{out(TIM-Mode)} = \left[\frac{s^2 C_1 C_2 R_1 R_3 R_2 I_2 - S \alpha_{P1} \beta_1 C_1 R_3 R_2 I_1 + R_2 \alpha_{P1} \beta_1 \alpha_{P2} \beta_2 I_3}{s^2 C_1 C_2 R_1 R_3 + g_{m1} S C_1 R_3 R_2 \alpha_{P1} \beta_1 \gamma_1 + \alpha_{P2} \beta_2 \gamma_2 \alpha_{P1} \beta_1 R_2 g_{m2}} \right] \tag{19}$$

$$f_0' = \frac{1}{2\pi}\sqrt{\frac{\alpha_{P2}\beta_2 Y_2 \alpha_{P1}\beta_1 R_2 g_{m2}}{C_1 C_2 R_3 R_1}} \quad (20)$$

$$Q' = \frac{1}{Y_1 g_{m1}}\sqrt{\frac{\alpha_{P2}\beta_2 C_2 Y_2 g_{m2} R_1}{\alpha_{P1}\beta_1 C_1 R_2 R_3}} \quad (21)$$

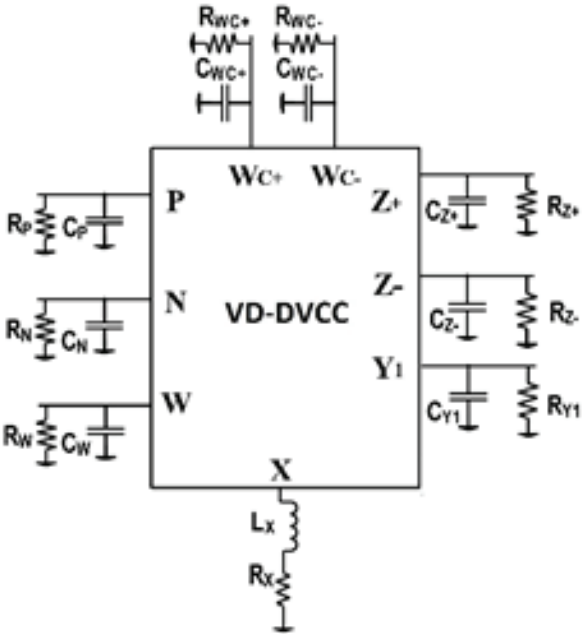

Figure 4: Non-ideal model of VD-DVCC with parasitics

The sensitivities of ω_0' and Q' with respect to the non-ideal gains and passive components are given below.

$$S_{g_{m2}}^{\omega_o'} = S_{\alpha_{P2}}^{\omega_o'} = S_{\beta_2}^{\omega_o'} = S_{\alpha_{P1}}^{\omega_o'} = S_{\beta 1}^{\omega_o'} = S_{R_2}^{\omega_o'} = S_{\gamma_2}^{\omega_o'} = -S_{C_1}^{\omega_o'} = -S_{C_2}^{\omega_o'} = -S_{R_3}^{\omega_o'} = -S_{R_1}^{\omega_o'} = \frac{1}{2} \quad (22)$$

$$S_{\alpha_{P2}}^{Q'} = S_{\beta_2}^{Q'} = -S_{C_1}^{Q'} = S_{\gamma_2}^{Q'} = S_{g_{m2}}^{Q'} = S_{C_2}^{Q'} = -S_{\alpha_{P1}}^{Q'} = -S_{\beta_1}^{Q'} = S_{R_1}^{Q'} = -S_{R_3}^{Q'} = -S_{R_2}^{Q'} = \frac{1}{2'} \quad (23)$$

$$-S_{\gamma_1}^{Q'} = -S_{g_{m1}}^{Q'} = 1, \quad (24)$$

The sensitivities are low and have absolute values not higher than unity.

5 Simulation and validation

To verify the proposed mixed-mode filter it is designed and simulated in Cadence virtuoso design software. The newly proposed VD-DVCC is designed in 0.18 µm Silterra Malaysia technology at a supply voltage of ±1V. The width and length of the transistors used are given in Table 4. The bias current of the OTA is fixed at 47 µA resulting in transconductance of 500 µS. The layout of the VD-DVCC is given in Figure 5 it occupies an area of 50.2*21.50µm^2.

Table 4: Width and Length of the MOS transistors

Transistors	Width (µm)	Length (µm)
M1-M4	4.5	0.36
M5-M6	20	0.36
M7-M8, M13	17.5	0.36
M14-M15	8.75	0.36
M9-M10	8.75	0.36
M11-M12, M16	13.5	0.36
M17-M18	17.5	0.36
M19-M20	1.8	0.36
M21-M25, M29-M30	3	0.72
M26-M28, M31-M32	8	0.36

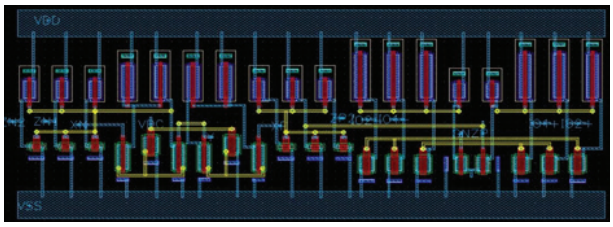

Figure 5: The complete layout of the VD-DVCC

The filter is designed for centre frequency of 5.305 MHz and quality factor of 1 by selecting passive component as $R_1 = R_2 = R_3 = 2\text{k}\Omega$ $C_1 = C_2 = 15\text{pF}$ and $g_m = 500$ µS. The power dissipation of the filter is found to be 3.48 mW. All five filter responses in VM, CM, TAM and TIM modes are presented in Figures 6-13.

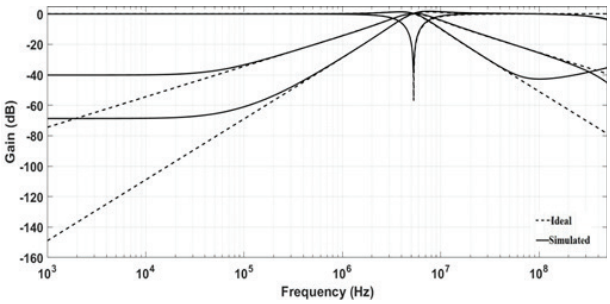

Figure 6: VM MISO configuration: Frequency responses of the LP, BP, HP, and BR filter

To examine the signal processing capability of the proposed universal filter the transient analysis is carried out in VM mode for HP, LP, NP and BP responses. A VM

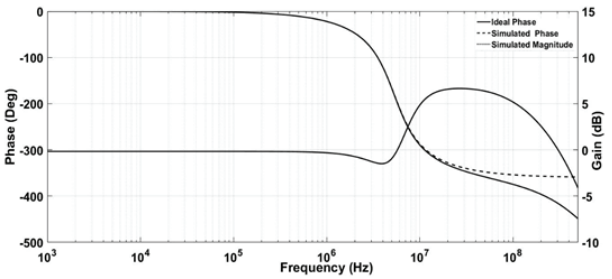

Figure 7: VM MISO configuration: Gain and phase responses of the AP filter

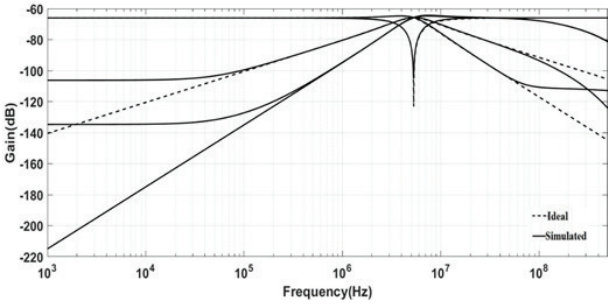

Figure 8: TAM MISO configuration: Frequency responses of the LP, BP, HP, and BR filter

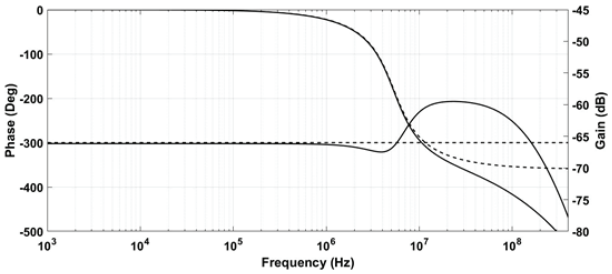

Figure 9: TAM MISO configuration: Gain and phase responses of the AP filter

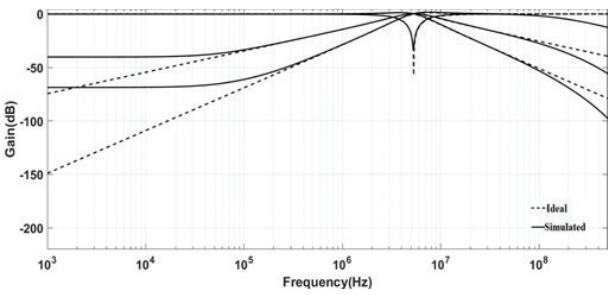

Figure 10: CM MISO configuration: Frequency responses of the LP, BP, HP, and BR filter

sinusoidal signal of 100 mV p-p and 5.305 MHz frequency is applied at the input and the output is analysed as presented in Figure 14. Similarly, a CM sinusoidal signal of 50 µA p-p and 5.305 MHz frequency is applied at the input and the BP output in CM and TIM is observed as shown in Figure 15. It can be inferred from figures that the filter works correctly.

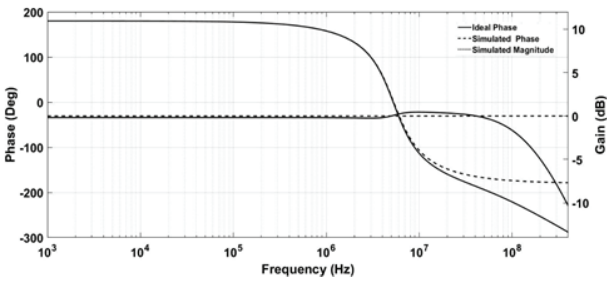

Figure 11: CM MISO configuration: Gain and phase responses of the AP filter

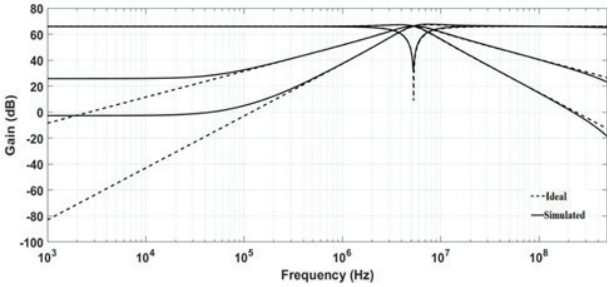

Figure 12: TIM MISO configuration: Frequency responses of the LP, BP, HP, and BR filter

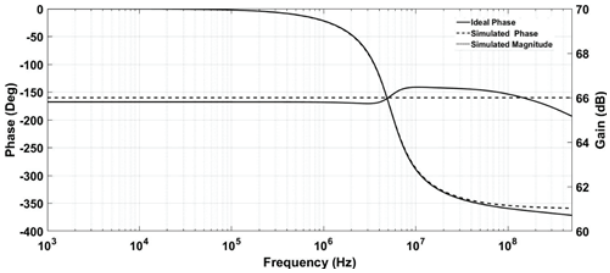

Figure 13: TIM MISO configuration: Gain and phase responses of the AP filter

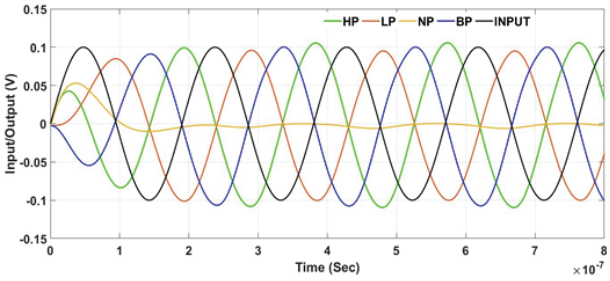

Figure 14: VM MISO configuration: Transient analysis results for BP, HP, LP filter configurations

In the presented filter the quality factor can be set independent of the pole frequency of the filter. The tunability of the quality factor is verified by analysing BP response in CM and TIM for different values of bias current IBIAS1 as shown in Figures 16-17. It can be deduced from figures that the quality factor of the filter can be tuned independent of the frequency.

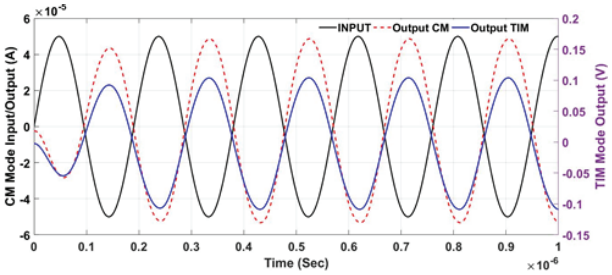

Figure 15: CM/TIM MISO configuration: Transient analysis results for BP filter configuration

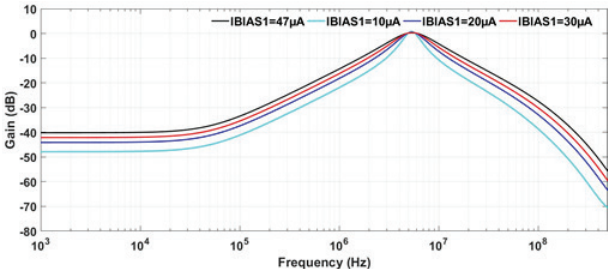

Figure 16: CM MISO configuration: Quality factor tuning for different values of OTA bias current

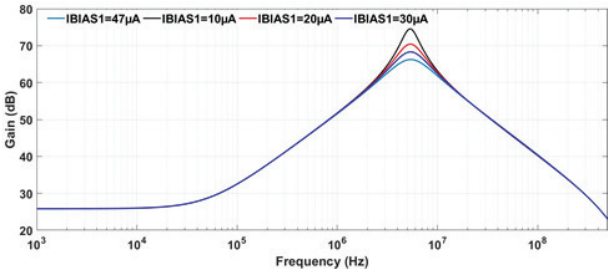

Figure 17: TIM MISO configuration: Quality factor tuning for different values of OTA bias current in BP filter

To study the effect of process spread on the performance of the designed filter Mont Carlo analysis is carried out for 200 runs. The Mont Carlo analysis results for VM BP response are given in Figures 18 and 19. The results for TIM AP configuration are given Figures 20 and 21.

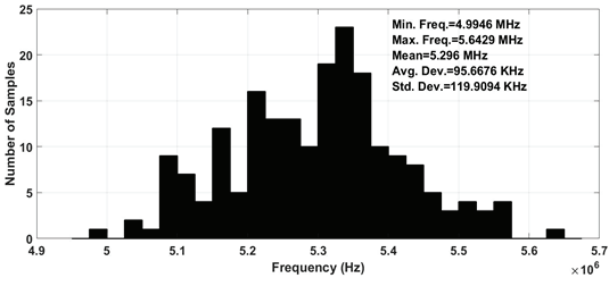

Figure 18: VM MISO configuration: The Monte Carlo analysis results for BP response

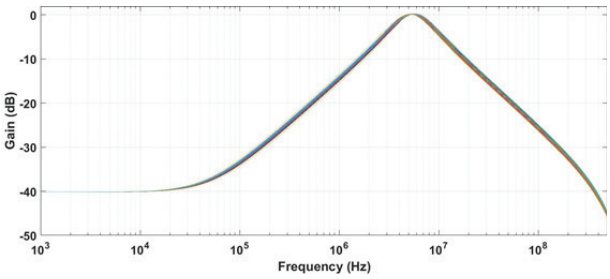

Figure 19: VM MISO configuration: The Monte Carlo analysis results for BP configuration

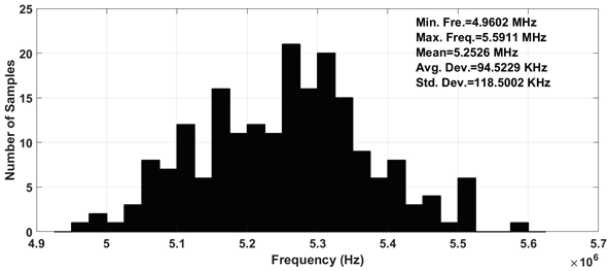

Figure 20: TIM MISO configuration: The Monte Carlo analysis results for AP response

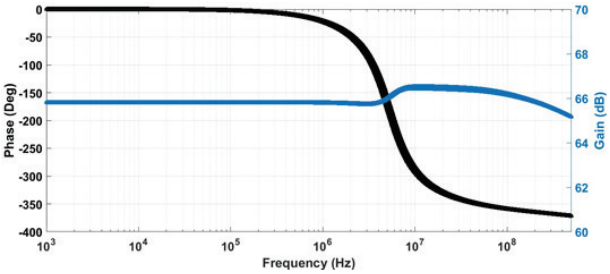

Figure 21: TIM MISO configuration: The Monte Carlo analysis results for AP configuration

The total harmonic distortion (THD) of the filter for LP and BP responses is plotted for different input signal amplitudes for VM as shown in Figure 22. The THD plot for CM-BP is presented in Figure 23. The THD remains within acceptable limits (≤5%) for appreciable input range.

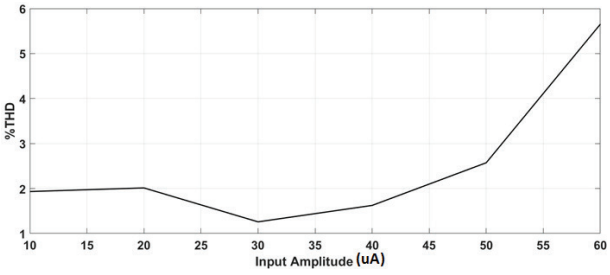

Figure 22: Total harmonic distortion of VM-BP and VM-LP

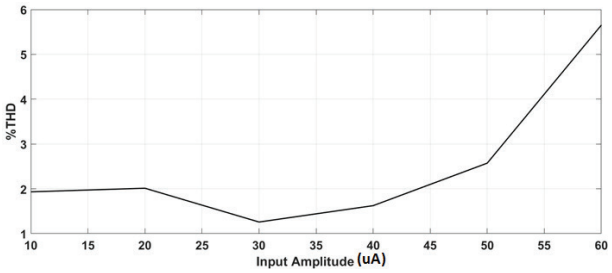

Figure 23: Total harmonic distortion of CM-BP

The pole frequency of the filter decreases due to rise in temperature Figure 24 because of the decrease in OTA transconductance. Two main contributing factors that influence the transconductance are the threshold voltage (V_t) and carrier mobility V_t. is approximated as a linear function of temperature [42,43] given by Equation 25. Where $\boldsymbol{\alpha}_{Vt}$ denotes the threshold voltage temperature coefficient which varies from −1 mV/ °C to −4 mV/ °C and T_O is the reference temperature (300 K).

$$V_t(T) = V_t(T_O) + \alpha_{Vt}(T - T_O) \tag{25}$$

The dependence of carrier mobility on temperature is shown in [42-43].

$$\mu_N(T) = \mu_N(T_O)\left(\frac{T}{T_O}\right)^{\alpha_\mu} \tag{26}$$

where, $\boldsymbol{\alpha}_{\boldsymbol{\mu}}$ is the mobility temperature exponent considered as a constant approximately equal to 1.5. The Equations (25) and (26), show that the threshold voltage (V_t) and mobility ($\boldsymbol{\mu}_N$) exhibit a negative temperature dependence.

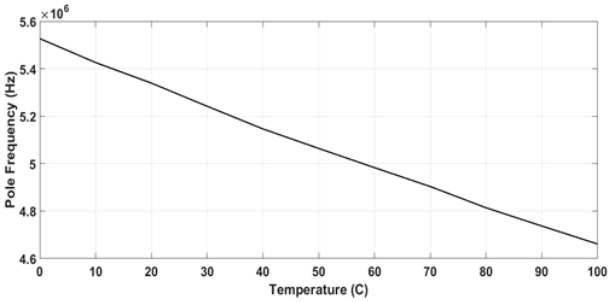

Figure 24: Variation of Filter Pole frequency with temperature

The input and output noise of the filter for VM-LP configuration is shown in Figure 25. The input referred noise magnitude for the VM-LP is found to be below 0.2E-06 $V/Hz^{1/2}$ till 10 MHz frequency. The maximum magnitude of output referred noise is 3.62E-08 $V/Hz^{1/2}$.

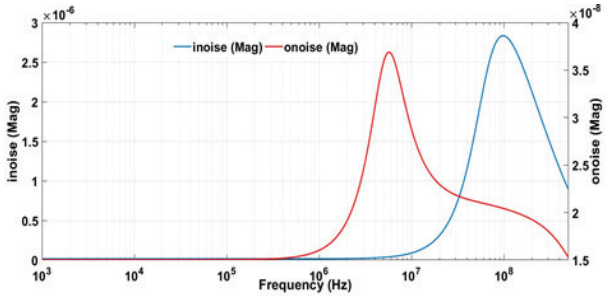

Figure 25: Input and output referred noise for VM-LP filter configuration

To further highlight the merits of the designed filter its performance is compared with some exemplary mixed mode filters as presented in Table 6. It can be observed that filters [46-47] cannot work in all four modes. The filters [24, 47] requires negative/double inputs for response realization. The filters structures [24,38,45] requires excessive numbers of ABBs for the design. It can be inferred from the table that the proposed filter has performance comparable with the existing designs. The power dissipation of the proposed filter can be reduced by designing the VD-DVCC for low supply operation.

6 Conclusion

This paper presents a new VD-DVCC based electronically tunable mixed-mode filter structure. The filter employs two VD-DVCCs, three grounded resistors and two grounded capacitors. Presented MISO filter has inbuilt tunability and can realize all five filter responses in all four modes of operation (VM, CM, TAM, and TIM). The detailed theoretical analysis, non-ideal gain analysis, and parasitic study are given. The VD-DVCC is designed in Cadence Virtuoso software and extensive simulations are carried out to examine and validate the proposed filter in all four mode of operation. The proposed filter has all the advantages mentioned in (i)-(iv). The filter is designed for a frequency of 5.305 MHz with ±1V supply. The power dissipation of the filter stands at 3.48 mW. The Monte Carlo analysis shows that the frequency deviation is within acceptable limits. Furthermore, the THD is within 5% for considerable voltage/current input signal range. The simulation results are found to be consistent with the theoretical predictions.

7 Acknowledgement

Part of this work was carried out at Institute of Microengineering and Nanoelectronics (IMEN),
University Kebangsaan Malaysia (UKM). This work is

funded by Ministry of Education Malaysia under grant (FRGS/1/2018/TK04/UKM/02/1) and AKU254:HICoE (Fasa II) 'MEMS for Biomedical Devices (artificial kidney)'.

8 References

1. P. A. Mohan, *Current-mode VLSI analog filters: design and applications*: Springer Science & Business Media 2012.
2. G. Ferri and N. C. Guerrini, *Low-voltage low-power CMOS current conveyors*: Springer Science & Business Media 2003.
3. R. Senani, D. Bhaskar, and A. Singh, *Current conveyors: variants, applications and hardware implementations*: Springer 2014.
4. M. Faseehuddin, J. Sampe, S. Shireen, and S. H. M. Ali, Minimum passive components based lossy and lossless inductor simulators employing a new active block, *AEU-Int. J. Electron. Commun.* **82** (2017) 226-240.
5. R. Raut and M. N. Swamy, *Modern analog filter analysis and design: a practical approach*: John Wiley & Sons 2010.
6. M. T. Abuelma'atti and A. Bentrcia, A novel mixed-mode CCII-based filter, *Act. and Passive Electron. Comp.* **27** (1970).
7. M. T. Abuelma'atti, A. Bentrcia, and S. A. M. Al-Shahrani, A novel mixed-mode current-conveyor-based filter, *Int. J. Electron.* **91** (2004) 191-197.
8. M. T. Abuelma'atti, A novel mixed-mode current-controlled current-conveyor-based filter, *J. Act. Passive Electron. Devices* **26** (2003) 185-191.
9. M. T. Abuelma'atti and A. Bentrcia, A novel mixed-mode OTA-C filter, *Frequenz* **57** (2003) 157-159.
10. R. Senani, Novel mixed-mode universal biquad configuration, *IEICE Electronics Express* **2** (2005), 548-553.
11. N. A. Shah and M. A. Malik, Multifunction mixed-mode filter using FTFNs, *Analog Integr. Circuits Signal Process.* **47** (2006) 339-343.
12. N. Pandey, S. K. Paul, A. Bhattacharyya, and J. SB, A new mixed mode biquad using reduced number of active and passive elements, *IEICE Electronics Express* **3** (2006), 115-121.
13. M. A. Ibrahim, Design and analysis of a mixed-mode universal filter using dual-output operational transconductance amplifiers (DO-OTAs), *International Conference on Computer and Communication Engineering* 2008 915-918.
14. C.-N. Lee and C.-M. Chang, Single FDCCII-based mixed-mode biquad filter with eight outputs, *AEU-Int. J. Electron. Commun.* **63** (2009) 736-742.
15. L. Zhijun, Mixed-mode universal filter using MCCCII, *AEU-Int. J. Electron. Commun.* **63** (2009) 1072-1075.
16. S. Minaei and M. A. Ibrahim, A mixed-mode KHN-biquad using DVCC and grounded passive elements suitable for direct cascading, *Int. J. Circuit Theory Appl.* **37** (2009) 793-810.
17. H.-P. Chen, Y.-Z. Liao, and W.-T. Lee, Tunable mixed-mode OTA-C universal filter, *Analog Integr. Circuits Signal Process.* **58** (2009) 135-141.
18. S. Maheshwari, S. V. Singh, and D. S. Chauhan, Electronically tunable low-voltage mixed-mode universal biquad filter, *IET cir., dev. & sys.* **5** (2011) 149-158.
19. C.-N. Lee, Multiple-mode OTA-C universal biquad filters, *Circuits Syst. Signal Process.* **29** (2010) 263-274.
20. N. Pandey, S. K. Paul, A. Bhattacharyya, and S. Jain, Realization of Generalized Mixed Mode Universal Filter Using CCCIIs, *J. Act. Passive Electron. Devices* **5** (2010).
21. S. Singh, S. Maheshwari, and D. Chauhan, Electronically tunable current/voltage-mode universal biquad filter using CCCCTA, *International J. of Recent Trends in Engineer. and Tech.* **3** (2010) 71-76.
22. W.-B. Liao and J.-C. Gu, SIMO type universal mixed-mode biquadratic filter, *Indian J. Eng. Mater. Sci.* **18** (2011) 443-448.
23. M. Kumngern and S. Junnapiya, Mixed-mode universal filter using OTAs, *IEEE International Conference on Cyber Technology in Automation, Control, and Intelligent Systems (CYBER)* 2012 119-122.
24. N. Pandey and S. K. Paul, Mixed mode universal filter, *J. Circuits Syst. Comput.* **22** (2013) 1250064.
25. F. Kaçar, A. Kuntman, and H. Kuntman, Mixed-mode biquad filter employing single active element, *IEEE 4th Latin American Symposium on Circuits and Systems* (2013) 1-4.
26. A. Yeşil and F. Kaçar, Electronically tunable resistorless mixed mode biquad filters, *Radioengineering* **22** (2013) 1016-1025.
27. E. Yuce, Fully integrable mixed-mode universal biquad with specific application of the CFOA, *AEU-Int. J. Electron. Commun* **64** (2010) 304-309.
28. L. Wang, C. Wang, J. Zhang, X. Liang, and S. Jiang, A new mixed-mode filter based on MDDCCs, *Seventh International Conference on Graphic and Image Processing* (2015) 981717.
29. C.-N. Lee, Independently tunable mixed-mode universal biquad filter with versatile input/output functions, *AEU-Int. J. Electron. Commun.* **70** (2016) 1006-1019.
30. C.-N. Lee, Mixed-mode universal biquadratic filter with no need of matching conditions, *J. Circuits Syst. Comput.* **25** (2016)C1650106.
31. H.-P. Chen and W.-S. Yang, Electronically tunable current controlled current conveyor transconductance amplifier-based mixed-mode biquad-

ratic filter with resistorless and grounded capacitors, *Applied Sciences* **7** (2017) 244.
32. V. Chamnanphrai and W. Sa-ngiamvibool, Electronically tunable SIMO mixed-mode universal filter using VDTAs, *Przegląd Elektrotechniczny* **93** (2017), 207-211.
33. M. Parvizi, A. Taghizadeh, H. Mahmoodian, and Z. D. Kozehkanani, A Low-Power Mixed-Mode SIMO Universal Gm–C Filter, *J. Circuits Syst. Comput.* **26** (2017) 1750164.
34. J.-W. Horng, C.-M. Wu, and N. Herencsar, Current-mode and transimpedance-mode universal biquadratic filter using two current conveyors, India J. of Engineer. & Mate. Sci. **24** (2017) 461-468.
35. U. Cini and M. Aktan, Dual-mode OTA based biquadratic filter suitable for current-mode applications, *AEU-Int. J. Electron. Commun.* **80** (2017) 43-47.
36. B. Chaturvedi, J. Mohan, and A. Kumar, A new versatile universal biquad configuration for emerging signal processing applications, *J. Circuits Syst. Comput.* **27** (2018) 1850196.
37. T. Tsukutani and N. Yabuki, A DVCC-Based Mixed-Mode Biquadratic Circuit," *J. of Electr. Engineer.* **6** (2018) 52-56.
38. D. R. Bhaskar, A. Raj, and P. Kumar, Mixed-Mode Universal Biquad Filter Using OTAs, *J. Circuits Syst. Comput.* **29** (2020) 2050162.
39. W.-C. Y. Chen-Nong Lee, General Mixed-Mode Single-Output DDCC-based Universal Biquad Filter, *Int. J. Eng. Res.* **9** (2020) 744-749.
40. T. Ettaghzouti, N. Hassen, and K. Besbes, "A Novel Multi-Input Single-Output Mixed-Mode Universal Filter Employing Second Generation Current Conveyor Circuit," *Sensors, Circuits & Instrumentation Systems: Extended Papers* **6** (2018), 53-63.
41. H.O. Elwan and A.M. Soliman, Novel CMOS differential voltage current conveyor and its applications, *IEE Proceedings-Circuits, Devices and Systems*, **144** (1997) 195-200.
42. Y. Tsividis and C. McAndrew, *Operation and Modeling of the MOS Transistor*: Oxford Univ. Press 2011.
43. I. Filanovsky and A. Allam, Mutual compensation of mobility and threshold voltage temperature effects with applications in CMOS circuits, *IEEE Trans. Circuits Syst. I, Fundam. Theory Appl.* **48** (2001) 876-884.
44. Lee, Chen-Nong, Mixed-mode universal biquadratic filter with no need of matching conditions, *J. Circuits Syst. Comput.* **25** (2016) 1650106.
45. M. Parvizi, A.Taghizadeh, H. Mahmoodian and Z.D. Kozehkanani, A Low-Power Mixed-Mode SIMO Universal Gm–C Filter, *J. Circuits Syst. Comput.* **26** (2017) 1750164.
46. U. Cini and M. Aktan, Dual-mode OTA based biquadratic filter suitable for current-mode applications, *AEU-Int. J. Electron. Commun.* **80** (2017) 43-47.
47. D. Agrawal and S. Maheshwari, High-Performance Electronically Tunable Analog Filter Using a Single EX-CCCII, *Circuits Syst. Signal Process.* 2020 https://doi.org/10.1007/s00034-020-01530-7.
48. Albrni MI, Mohammad F, Herencsar N, Sampe J, Ali SH. Novel electronically tunable biquadratic mixed-mode universal filter capable of operating in MISO and SIMO configurations. Inf. MIDEM. 2020 Jul;50:189-203.
49. Faseehuddin M, Herencsar N, Albrni MA, Shireen S, Sampe J. Electronically tunable mixed mode universal filter employing grounded capacitors utilizing highly versatile VD-DVCC. Circuit World. 2021.
50. Roongmuanpha N, Faseehuddin M, Herencsar N, Tangsrirat W. Tunable Mixed-Mode Voltage Differencing Buffered Amplifier-Based Universal Filter with Independently High-Q Factor Controllability. Applied Sciences. 2021,11(20):9606.
51. Faseehuddin M, Herencsar N, Shireen S, Tangsrirat W, Md Ali SH. Voltage Differencing Buffered Amplifier-Based Novel Truly Mixed-Mode Biquadratic Universal Filter with Versatile Input/Output Features. Applied Sciences. 2022,12(3):1229.
52. Faseehuddin M, Herencsar N, Albrni MA, Sampe J. Electronically tunable mixed-mode universal filter employing a single active block and a minimum number of passive components. Applied Sciences. 2020,11(1):55.

Arrived: 09. 04. 2022
Accepted: 22 .06. 2022